multimedia

Single-cell imaging of graded Ins(1,4,5)P_3 production following G-protein-coupled-receptor activation

Mark S. NASH[1], Kenneth W. YOUNG, Gary B. WILLARS, R. A. John CHALLISS and Stefan R. NAHORSKI

*Department of Cell Physiology and Pharmacology, Medical Sciences Building, University of Leicester, P.O. Box 138, University Road, Leicester LE1 9HN, U.K.

The pleckstrin homology domain of phospholipase Cδ1 ($PH_{PLC\delta}$) binds Ins(1,4,5)P_3 and PtdIns(4,5)P_2 specifically, and can be used to detect changes in Ins(1,4,5)P_3 in single cells. A fusion construct of $PH_{PLC\delta}$ and enhanced green fluorescent protein (EGFP–$PH_{PLC\delta}$) associates with the plasma membrane due to its association with PtdIns(4,5)P_2. However, $PH_{PLC\delta}$ has greater affinity for Ins(1,4,5)P_3 than PtdIns(4,5)P_2, and translocates to the cytosol as Ins(1,4,5)P_3 levels rise. Prolonged activation of group I metabotropic glutamate receptor 1α expressed in Chinese-hamster ovary cells or endogenous M_3 muscarinic receptors in SH-SY5Y neuroblastoma cells gave an initial transient peak in translocation, followed by a sustained plateau phase. This closely followed changes in cell population Ins(1,4,5)P_3 mass, but not PtdIns(4,5)P_2 levels, which decreased monophasically, as determined by radioreceptor assay. Translocation thus provides a real-time method to follow increases in Ins(1,4,5)P_3. Graded changes in Ins(1,4,5)P_3 in Chinese-hamster ovary-lac-mGlu1α cells could be detected with increasing glutamate concentrations, and dual loading with fura 2 and EGFP–$PH_{PLC\delta}$ showed that changes in intracellular Ca^{2+} concentration closely paralleled Ins(1,4,5)P_3 production. Moreover, Ins(1,4,5)P_3 accumulation and intracellular Ca^{2+} mobilization within single cells is graded in nature and dependent on both agonist concentration and receptor density.

Key words: group I metabotropic glutamate receptor 1α, M_3 muscarinic receptor, pleckstrin homology domain.

INTRODUCTION

The ability to determine intracellular calcium concentrations ($[Ca^{2+}]_i$) in single cells has had a profound effect on our understanding of the dynamics of G-protein-coupled-receptor (GPCR)-stimulated mobilization of intracellular calcium (Ca^{2+}_i) stores. Imaging techniques have made it possible to visualize oscillations in $[Ca^{2+}]_i$ [1,2], observe subcellular events in Ca^{2+} release [3–5] and to establish that release of calcium from intracellular stores is 'quantal', i.e. graded in response rather than 'all-or-none' [6–10]. Unfortunately, the inability to visualize single-cell Ins(1,4,5)P_3 has meant that assumptions must be made regarding the relationship between Ins(1,4,5)P_3 production and $[Ca^{2+}]_i$ mobilization. Thus models of quantal Ca^{2+} release are often based upon studies where Ins(1,4,5)P_3 concentration is increased directly by external addition or uncaging [7,8,10]. However, this presupposes that stepwise increases in GPCR activation result in graded phospholipase C (PLC) activity and hence graded production of Ins(1,4,5)P_3. Population-based biochemical assays cannot yield accurate temporal data on changes in Ins(1,4,5)P_3 concentration, or prove conclusively that Ins(1,4,5)P_3 production is graded within each cell. It remains possible that PLC activity following agonist challenge is effectively 'all-or-none' due to amplification involving, for example, Ca^{2+} feed-forward on Ca^{2+}-dependent PLCs [11–13]. Concentration-dependence observed biochemically might also reflect an all-or-none response in a variable number of cells. We have attempted to address this fundamental issue by following Ins(1,4,5)P_3 production in single cells.

Recent developments to track the subcellular localization of green fluorescent protein (GFP)-tagged proteins with high selectivity for intracellular messengers now make it possible to image cellular levels of Ins(1,4,5)P_3 in real time in single cells [14–16]. The pleckstrin homology domain of PLCδ1 ($PH_{PLC\delta}$) binds with high affinity and selectivity to PtdIns(4,5)P_2 [17], and a fusion construct of $PH_{PLC\delta}$ with enhanced GFP (EGFP–$PH_{PLC\delta}$) enriches over the plasma membrane through this association [14–16]. Recently [16], $PH_{PLC\delta}$ was found to show approx. 20-fold greater affinity for the soluble head-group of PtdIns(4,5)P_2, i.e. Ins(1,4,5)P_3, using a surface plasmon assay. Moreover, intracellular injection of Ins(1,4,5)P_3 elicited translocation of the fusion protein to the cytosol, and co-transfection with the catabolic enzyme Ins(1,4,5)P_3 5-phosphatase prevented agonist-induced translocation [16]. The combined data suggest, therefore, that agonist-stimulated Ins(1,4,5)P_3 production is primarily responsible for translocation of EGFP–$PH_{PLC\delta}$, with little contribution of PtdIns(4,5)P_2 depletion as a result of PLC activity.

Using our knowledge of M_3 muscarinic receptor-induced changes in the levels of Ins(1,4,5)P_3 and its phosphoinositide precursor in SH-SY5Y neuroblastoma cells [18–20], we provide further evidence that the extent of membrane association of EGFP–$PH_{PLC\delta}$ reflects cellular Ins(1,4,5)P_3 levels. We have used this technique to study single-cell Ins(1,4,5)P_3 production following activation of a group I metabotropic glutamate receptor 1α (mGlu1α) heterologously expressed in Chinese-hamster ovary (CHO) cells [21,22]. In the present paper, we demonstrate for the first time that Ins(1,4,5)P_3 production is graded in response to changes in agonist concentration within individual cells and that

Abbreviations used: PLC, phospholipase C; $PH_{PLC\delta}$, pleckstrin homology domain of PLCδ1; EGFP, enhanced green fluorescent protein; mGlu1α, group I metabotropic glutamate receptor 1α; CHO, Chinese-hamster ovary; GPCR, G-protein-coupled receptor; $[Ca^{2+}]_i$, intracellular calcium concentration; IPTG, isopropyl β-D-thiogalactoside; KHB, Krebs–Henseleit buffer.

[1] To whom correspondence should be addressed (e-mail msn2@le.ac.uk).

levels closely correlate with changes in $[Ca^{2+}]_i$. We conclude that EGFP–$PH_{PLC\delta}$ translocation represents an excellent index to follow Ins(1,4,5)P_3 production and is likely to have a major impact on our understanding of GPCR-stimulated PLC activity.

EXPERIMENTAL

Vector containing the fusion construct between EGFP and the PH domain of PLCδ1 was kindly provided by Professor T. Meyer (Stanford University, CA, U.S.A.). Detailed information regarding this construct can be found in Stauffer et al. [14]. A description of the LacSwitch II-inducible expression system (Stratagene) used to express human mGlu1α receptor in CHO cells (CHO-lac-mGlu1α) [21], and a comprehensive pharmacological analysis of the endogenous M_3 muscarinic receptor expressed by SH-SY5Y cells [23,24], are provided elsewhere. Information regarding the culture conditions for the two cell types is given in the relevant references.

Single-cell measurement of Ins(1,4,5)P_3 was conducted on cells seeded on to 22 mm diameter borosilicate coverslips. Cells were incubated for 8 h and then transiently transfected with EGFP–$PH_{PLC\delta}$ plasmid DNA using FuGENE 6™ (1:3, w/v), as per manufacturer's instructions (Roche Diagnostics, Lewes, East Sussex, U.K.). For CHO-lac-mGlu1α cells, after 20 h the transfection medium was replaced with medium containing 100 μM isopropyl β-D-thiogalactoside (IPTG) and the cells were incubated for another 20 h. Cells were perfused (5 ml/min) with Krebs–Henseleit buffer (KHB; 10 mM Hepes/118 mM NaCl/4.69 mM KCl/10 mM glucose/1.18 mM KH_2PO_4/4.2 mM $NaHCO_3$/1.18 mM $MgCl_2$/1.3 mM $CaCl_2$, pH 7.4) using a Gilson Minipuls 2 pump connected to a coverslip chamber maintained at 37 °C using a Peltier unit, and confocal images were captured using an UltraVIEW LCI confocal system (Perkin Elmer). Drug solutions were either applied through the perfusion line or, for shorter (< 30 s) periods of challenge, directly perfused over the cells with the outflow and inflow perfusion lines open and closed respectively.

For dual imaging of Ins(1,4,5)P_3 and $[Ca^{2+}]_i$, transfected cells were also loaded with 5 μM fura 2 acetoxymethyl ester and mounted on the stage of a Nikon Diaphot inverted epifluorescence microscope. Sequential images were captured at wavelengths above 510 nm after excitation at 340, 380 and 490 nm using an intensified charge-coupled device camera (Photonic Science) connected to a Quanticell 700 (Applied Imaging, Sunderland, Tyne and Wear, U.K.) system. To analyse the EGFP–$PH_{PLC\delta}$ signal, an area within the cytoplasm was highlighted and the mean fluorescence recorded. The data are expressed as a ratio of fluorescence at a given time point to basal levels. $[Ca^{2+}]_i$ from the same region was determined as described previously [25].

Radioreceptor assays for quantification of Ins(1,4,5)P_3 mass and determination of PtdIns(4,5)P_2 levels in cell populations were performed as described by Willars et al. [20]. Statistical analysis was performed using Student's t test, and P values < 0.05 were considered statistically significant.

RESULTS

Transient transfection of CHO-lac-mGlu1α (Figure 1A) and SH-SY5Y (Figure 1C) cells with EGFP–$PH_{PLC\delta}$ resulted in a concentration of fluorescence over the plasma membrane representing the association of the fusion protein with PtdIns(4,5)P_2.

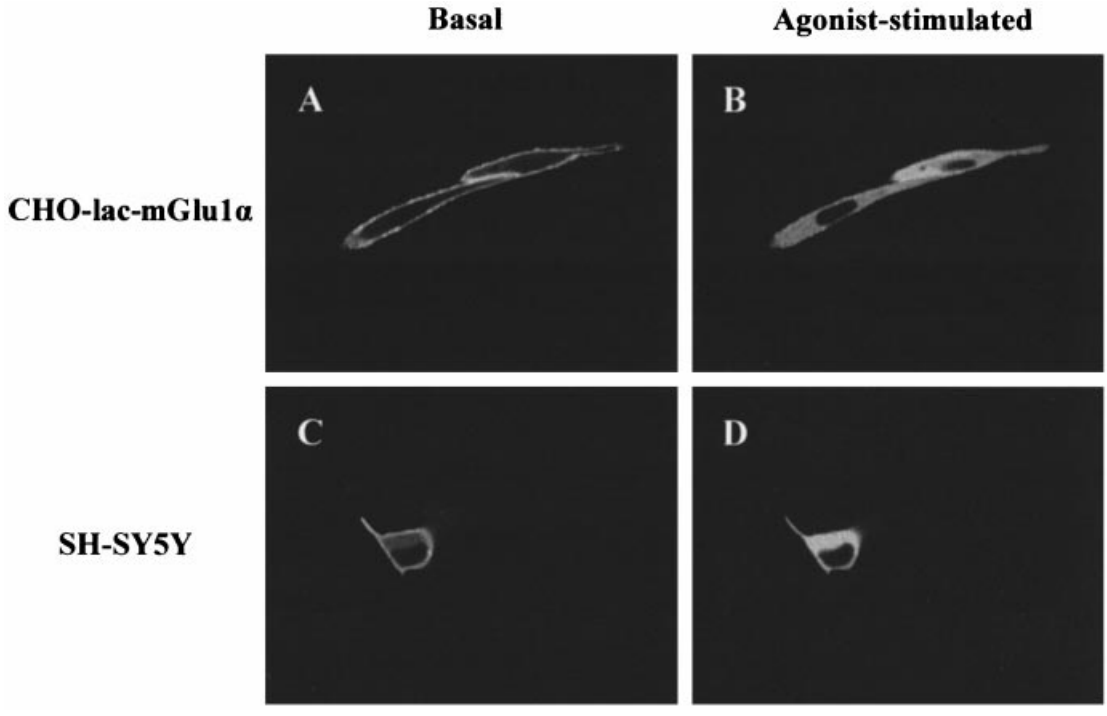

Figure 1 Confocal single-cell imaging of agonist-induced changes in EGFP–$PH_{PLC\delta}$ fluorescence in CHO-lac-mGlu1α and SH-SY5Y cells

CHO-lac-mGlu1α (**A**, **B**) and SH-SY5Y neuroblastoma (**C**, **D**) cells transiently transfected with EGFP–$PH_{PLC\delta}$ were perfused with either 1 mM glutamate or 1 mM carbachol respectively, and fluorescent images captured prior to (**A**, **C**) and approx 60 s after (**B**, **D**) drug challenge. An animation showing the change in cytosolic EGFP–$PH_{PLC\delta}$ fluorescence in CHO-lac-mGlu1α cells during glutamate application can be viewed at http://www.BiochemJ.org/bj/356/bj3560137add.htm.

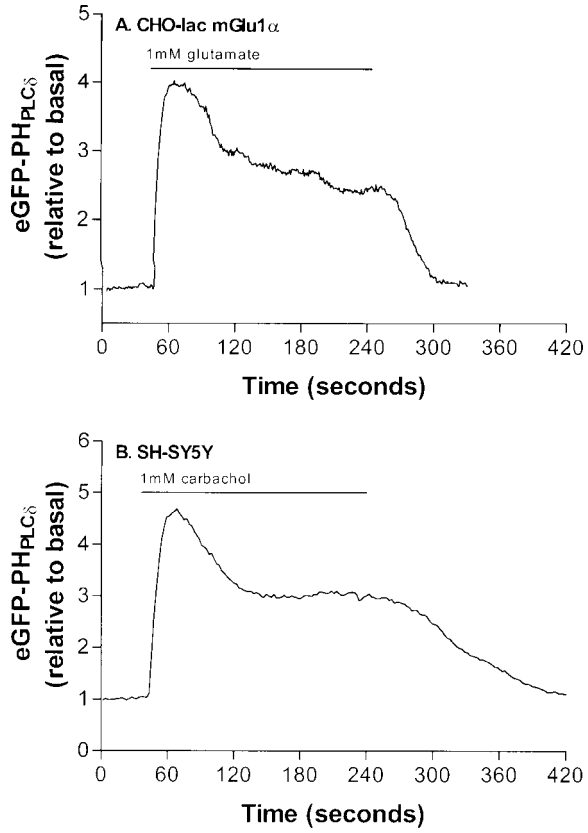

Figure 2 Effect of agonist challenge on cellular Ins(1,4,5)P_3 levels in single CHO-lac-mGlu1α (A) and SH-SY5Y neuroblastoma (B) cells

Representative traces from confocal imaging EGFP–PH$_{PLC\delta}$ fluorescence showing the effect on cytoplasmic levels relative to basal of prolonged stimulation of CHO-lac-mGlu1α (**A**) and SH-SY5Y neuroblastoma (**B**) cells with 1 mM glutamate and 1 mM carbachol respectively. Cells were transiently transfected with EGFP–PH$_{PLC\delta}$ 48 h prior to experimentation and receptor expression in the CHO-lac-mGlu1α cells induced with 100 μM IPTG for 20 h. The solid line indicates the period of drug application.

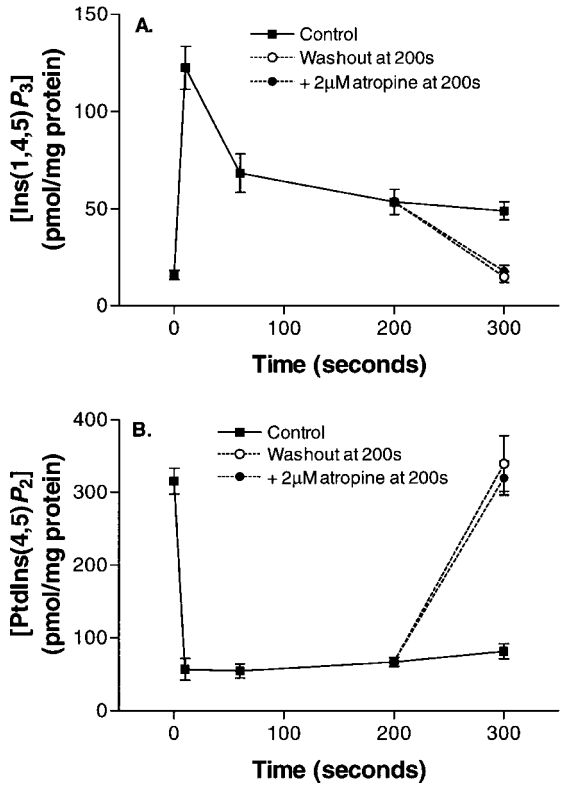

Figure 3 Comparison of the effect of carbachol on total Ins(1,4,5)P_3 and PtdIns(4,5)P_2 levels in SH-SY5Y cells

SH-SY5Y cells were exposed to 1 mM carbachol ($t = 0$) and incubated at 37 °C for various time periods. The effect on Ins(1,4,5)P_3 (**A**) and PtdIns(4,5)P_2 (**B**) levels was determined using radioreceptor mass assays. For some treatments, cells were exposed to carbachol for 200 s and the cells either washed or 2 μM atropine added. Data are expressed as means ± S.E.M. ($n = 5$).

Challenge with maximal concentrations of glutamate (Figure 1B) or carbachol (Figure 1D) resulted in a loss of membrane association and an enrichment of cytosolic fluorescence in CHO-lac-mGlu1α and SH-SY5Y cells, respectively. An animation showing the change in cytosolic EGFP–PH$_{PLC\delta}$ fluorescence in CHO-lac-mGlu1α cells during glutamate application can be viewed at http://www.BiochemJ.org/bj/356/bj3560137add.htm. Expression of the EGFP control plasmid in SH-SY5Y cells resulted in cytosolic fluorescence only, and this was unchanged following methacholine treatment (results not shown).

Plotting the change in cytosolic fluorescence against time during prolonged agonist challenge revealed a large initial peak followed by a lower sustained level in the CHO-lac-mGlu1α and SH-SY5Y cells (Figure 2). These changes in fluorescence ratio returned to basal levels after perfusion with KHB alone. This pattern is typical for the stimulation of Ins(1,4,5)P_3 production (Figure 3A), quantified using a radioreceptor assay, following activation of M_3 muscarinic receptors in populations of SH-SY5Y cells where agonist was either washed out or 2 μM atropine added. In contrast, levels of PtdIns(4,5)P_2 were found to decrease monophasically in the SH-SY5Y cells during agonist challenge, with no evidence of an inverted 'peak' and 'plateau' response (Figure 3B). Graded EGFP–PH$_{PLC\delta}$ translocation in CHO-lac-mGlu1α cells was obtained to increasing concentrations of glutamate applied for 30 s (Figures 4A and 4B), and the graded nature of the response was confirmed by the combined data from different cells (Figure 4C). Similar results were obtained in a separate series of experiments where glutamate was perfused over the cells for 3 min and peak responses determined (results not shown). An animated version of the experiment shown in Figure 4(A) can be viewed at http://www.BiochemJ.org/bj/356/bj3560137add.htm.

Dual measurement of Ins(1,4,5)P_3 concentration and $[Ca^{2+}]_i$ in glutamate-challenged CHO-lac-mGlu1α cells revealed the close relationship between these two consequences of PLC activation (Figure 5). The ratiometric values for EGFP–PH$_{PLC\delta}$ changes were less than those obtained previously (Figure 2) because interference from different focal planes increases the background fluorescence in these non-confocal experiments. Prolonged exposure to glutamate (1 mM) induced a peak and plateau in both Ins(1,4,5)P_3 concentration and $[Ca^{2+}]_i$ (Figure 5A). The changes in $[Ca^{2+}]_i$ were consistently observed to peak and reach sustained levels before those in Ins(1,4,5)P_3 concentration (Figure 5A), although it is possible that this may only reflect differences in the kinetics of the two detection methods. Concentration-dependency for both the initial peak height and plateau level (measured at 200 s) of glutamate-induced changes in Ins(1,4,5)P_3 and $[Ca^{2+}]_i$ were observed (Figure 5B). EC_{50} values of 7.4 μM and 3.3 μM for the peak Ins(1,4,5)P_3 and $[Ca^{2+}]_i$ response were obtained respectively, and similar values for the plateau levels of

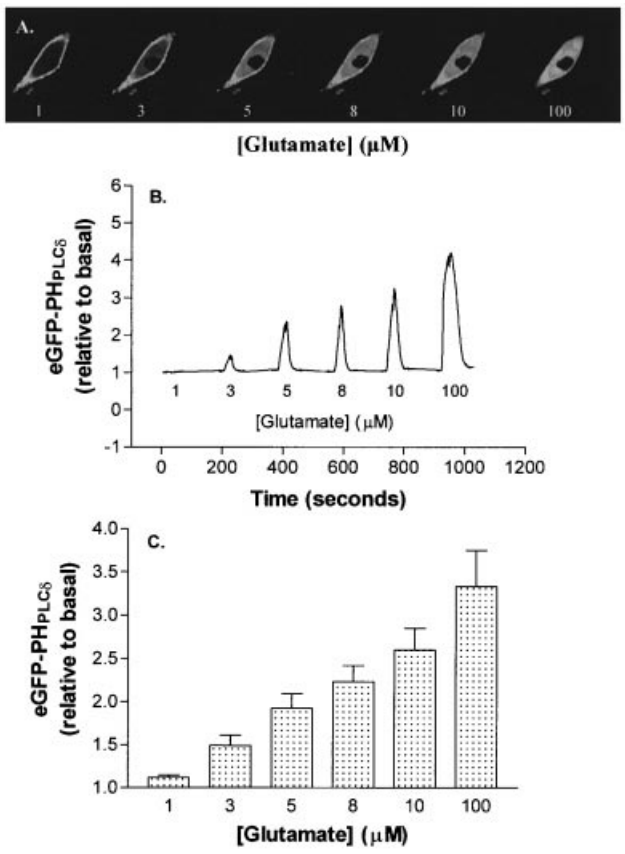

Figure 4 Effect of incremental glutamate concentrations on Ins(1,4,5)P_3 levels in single CHO-lac-mGlu1α cells

CHO-lac-mGlu1α cells were transiently transfected with EGFP–$PH_{PLC\delta}$ for 48 h and receptor expression induced with 100 μM IPTG for 20 h. A series of confocal images of a single cell were captured following repeated challenge for 30 s with increasing concentrations of glutamate (**A**). An animated version of (**A**) can be viewed at http://www.BiochemJ.org/bj/356/bj3560137add.htm. Cells were washed with KHB for 150 s between each treatment. The changes in cytosolic EGFP–$PH_{PLC\delta}$ fluorescence in this cell are plotted in (**B**) and the data averaged (means $\pm$ S.E.M.) for 10 separate cells from four independent experiments (**C**). Glutamate (100 μM) was determined to induce maximal responses in a separate series of experiments (results not shown).

Ins(1,4,5)P_3 (10.8 μM) and $[Ca^{2+}]_i$ (2.6 μM). Graded responses could also be detected when making dual measurements (Figure 5C). Application of 10 μM glutamate to CHO-lac-mGlu1α cells induced a peak Ins(1,4,5)P_3 accumulation of 1.13 ± 0.02 ($n = 14$; change in cytosolic EGFP–$PH_{PLC\delta}$ fluorescence, arbitary units) and a peak of 415 ± 56 nM above basal in $[Ca^{2+}]_i$. The same cells challenged with 1 mM glutamate responded with a peak of 1.23 ± 0.03 ($P < 0.001$ compared with 10 μM) in Ins(1,4,5)P_3 accumulation and a 551 ± 35 nM ($P < 0.01$) increase above basal in $[Ca^{2+}]_i$. Repeated application of glutamate (1 mM) for 3 s interspersed with 30 s washes demonstrated how closely the changes in $[Ca^{2+}]_i$ and Ins(1,4,5)P_3 concentration paralleled each other (Figure 5D).

Using the inducible LacSwitch II-expression system, the levels of mGlu1α receptor present in the CHO-lac-mGlu1α cells can be controlled by simply varying the IPTG concentration [21,22]. Challenging cells exposed to IPTG for 20 h with 1 mM glutamate gave changes in both peak and plateau Ins(1,4,5)P_3 concentration (Figure 6A) and $[Ca^{2+}]_i$ (Figure 6B), the magnitude of which varied according to the concentration of IPTG used to induce receptor expression. Half-maximal values for the induction of peak Ins(1,4,5)P_3 concentration and $[Ca^{2+}]_i$ responses by IPTG were 20 μM and 7 μM respectively. Plateau EC_{50} values were 22 μM and 5 μM for Ins(1,4,5)P_3 concentration and $[Ca^{2+}]_i$ respectively. Thus the extent of Ins(1,4,5)P_3 production and $Ca^{2+}{}_i$ mobilization is determined not only by agonist concentration, but also by the level of expression of the receptor. Moreover, the relationship between the two parameters remains similar as receptor density decreases.

DISCUSSION

The crucial finding of the present work is that increasing activation of either M_3 muscarinic or mGlu1α receptors leads to finely graded increases in Ins(1,4,5)P_3 levels within a single cell. Previously this could only be inferred from population-based biochemical assays, and the development of a single-cell based Ins(1,4,5)P_3 assay has allowed this issue to be directly addressed for the first time. There is already strong evidence that assessing translocation of the EGFP–$PH_{PLC\delta}$ fusion protein is monitoring changes in Ins(1,4,5)P_3 rather than measuring the loss of membrane PtdIns(4,5)P_2 due to hydrolysis by PLC [16]. Thus $PH_{PLC\delta}$ shows 20-fold higher affinity for Ins(1,4,5)P_3 than PtdIns(4,5)P_2, and intracellular injection of Ins(1,4,5)P_3 induces EGFP–$PH_{PLC\delta}$ translocation even in cells where $Ca^{2+}{}_i$ stores were depleted to eliminate the possibility of Ca^{2+}-induced PLC activation [16]. Furthermore, rapid catabolism of Ins(1,4,5)P_3 by transfection with an Ins(1,4,5)P_3 5-phosphatase abolished agonist-induced EGFP–$PH_{PLC\delta}$ translocation [16].

We have further addressed this issue by comparing EGFP–$PH_{PLC\delta}$ translocation in SH-SY5Y cells with experiments measuring changes in Ins(1,4,5)P_3 and PtdIns(4,5)P_2 mass using radioreceptor-based assays of which our laboratory has extensive experience [20]. With this knowledge, we postulated that the changes in subcellular localization of EGFP–$PH_{PLC\delta}$ would mimic most closely the changes in Ins(1,4,5)P_3 or PtdIns(4,5)P_2 that mediate translocation. The data demonstrated that changes in cytosolic EGFP–$PH_{PLC\delta}$ fluorescence most closely paralleled the biphasic response characteristic of Ins(1,4,5)P_3 levels rather than the monophasic changes in PtdIns(4,5)P_2 levels (Figures 2B and 3).

Overall, this provides compelling evidence that EGFP–$PH_{PLC\delta}$ allows us to follow the levels of Ins(1,4,5)P_3 in a single cell in real time. The observation that EGFP–$PH_{PLC\delta}$ partially returns to the membrane during the plateau phase, at a time when PtdIns(4,5)P_2 levels remain low, has an additional implication. It may indicate that despite the marked overall decrease in PtdIns(4,5)P_2 concentration, 'local' levels of this phosphoinositide are still sufficient for a predominant plasma membrane localization of EGFP–$PH_{PLC\delta}$. Therefore the level of EGFP–$PH_{PLC\delta}$ expression must be small compared with total PtdIns(4,5)P_2 concentration. This further suggests that significant sequestration of Ins(1,4,5)P_3 by binding to $PH_{PLC\delta}$ is unlikely, and argues that, in an analogous manner to the use of fluorescent Ca^{2+}-sensing dyes, levels of EGFP–$PH_{PLC\delta}$ used to detect signalling events do not significantly influence the magnitude of the changes.

The demonstration of graded Ins(1,4,5)P_3 production has important implications for the understanding of the phenomenon of quantal Ca^{2+} release. Thus in each cell a given agonist concentration elicits a defined and apparently finely tuned (Figure 4) amount of Ins(1,4,5)P_3 production. This sensitizes, in an Ins(1,4,5)P_3 concentration-dependent manner, a set number of Ins(1,4,5)P_3 receptors present on the endoplasmic reticulum, resulting in specific quantal Ca^{2+} release [26,27]. The magnitude of Ca^{2+} release will be determined by the extent of interaction of Ins(1,4,5)P_3 with its receptor, combined with the ability of Ca^{2+}

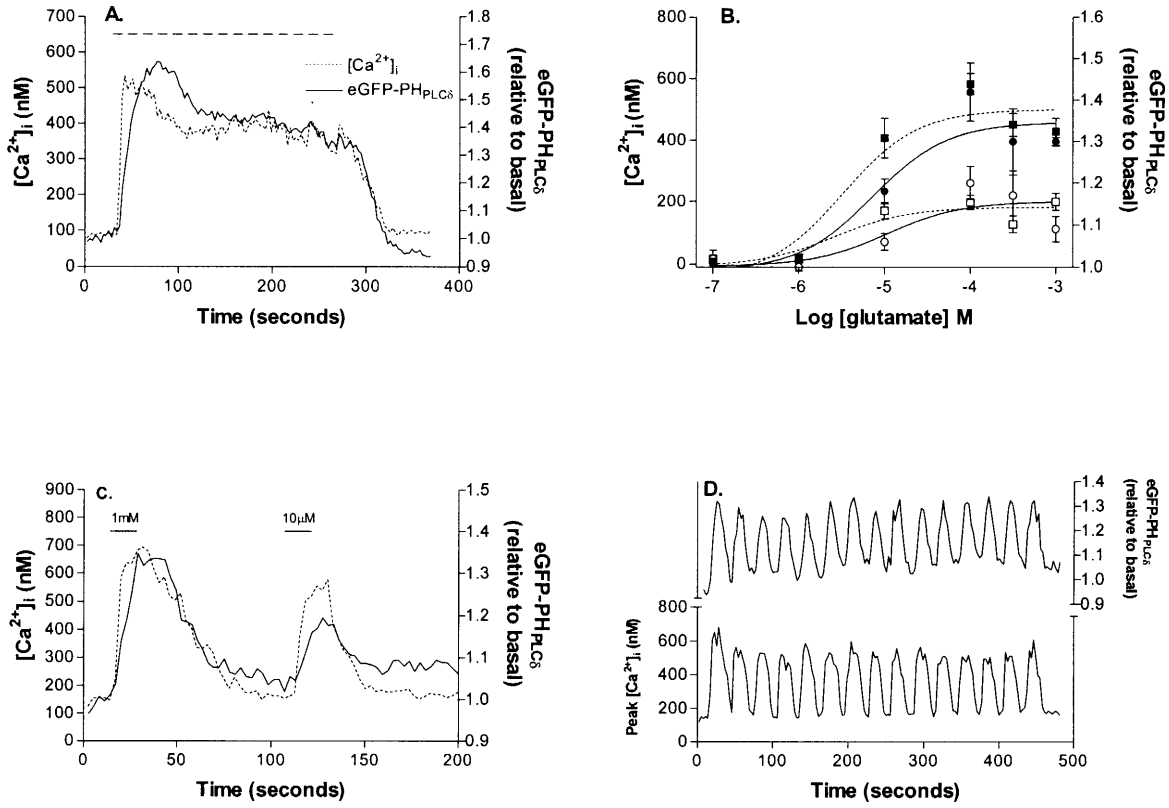

Figure 5 Co-detection of changes in Ins(1,4,5)P_3 and $[Ca^{2+}]_i$ levels in single CHO-lac-mGlu1α cells stimulated with glutamate

(**A**) Representative traces showing the simultaneous detection of changes in Ins(1,4,5)P_3 concentration (solid line) and $[Ca^{2+}]_i$ (dotted line) in a single CHO-lac-mGlu1α cell challenged with 1 mM glutamate (broken line). (**B**) Concentration-response curves for the effect of glutamate on peak (filled symbols) and plateau (open symbols) levels of Ins(1,4,5)P_3 (circles) and $[Ca^{2+}]_i$ (squares). A comparison of the changes in Ins(1,4,5)P_3 (solid line) and $[Ca^{2+}]_i$ (dashed line) levels induced by 1 mM glutamate with that for 10 μM glutamate is shown in (**C**). (**D**) The close relationship between Ins(1,4,5)P_3 (top line) and $[Ca^{2+}]_i$ (bottom line) following repeated challenge with 1 mM glutamate for 3 s interspersed with washing with KHB for 27 s.

once released to promote further Ca^{2+} mobilization through Ca^{2+}-induced Ca^{2+} release. Interestingly, increases in Ins(1,4,5)P_3 production are detectable over a relatively small range of agonist concentrations, such that relatively large variations can be observed between differences of a few μM. This is likely to be a consequence of feed-forward from the Ca^{2+} released from the intracellular stores on Ca^{2+}-activated PLCs (e.g. PLCδ [11–13]) and facilitation of agonist-activated PLCs [11]. Indeed, we have previously shown [28] that Ca^{2+} store-depletion by thapsigargin pretreatment causes attenuations of agonist-mediated Ins(1,4,5)P_3 responses to activation of M_3 muscarinic receptors.

Dual imaging of $[Ca^{2+}]_i$ and Ins(1,4,5)P_3 showed that there is a close relationship between these two parameters. Not only do changes in levels parallel each other during prolonged agonist stimulation, but also repeated challenges elicit concurrent effects on both cytosolic Ins(1,4,5)P_3 and Ca^{2+} levels. Moreover, graded changes in both Ins(1,4,5)P_3 concentration and $[Ca^{2+}]_i$ can be observed in CHO-lac-mGlu1α cells when the glutamate concentration is decreased. For the mGlu1α receptor we also show that there is little amplification of the response to glutamate between Ins(1,4,5)P_3 production and $[Ca^{2+}]_i$ release, since EC_{50} values differ by only 0.5 log unit. This contrasts markedly with M_3 muscarinic-induced changes in Ins(1,4,5)P_3 concentration and $[Ca^{2+}]_i$ in SH-SY5Y cells, where EC_{50} values differ by approx. 2.0 log units [18]. This is likely to reflect differences in the extent of amplification between Ins(1,4,5)P_3 production and $[Ca^{2+}]_i$ release in a cell- and receptor-dependent manner. The importance of receptor density on mGlu1α receptor responses was also highlighted by titrating expression in cells challenged with a high concentration of glutamate. These results compare favourably with the extent of IPTG-induced mGlu1α receptor protein expression observed by Western blotting and with agonist-induced changes in Ins(1,4,5)P_3 production determined using a radioreceptor assay [21,22].

The use of EGFP–$PH_{PLC\delta}$ translocation to monitor cellular Ins(1,4,5)P_3 levels has several clear advantages over traditional biochemical measurements made on cell populations. First, and most importantly, it provides data on single cells, and so gives the actual changes in each individual cell, rather than a summation of the effect on a population. This is crucial in order to distinguish between graded responses and changes in synchronicity, or in the number of responding cells. A corollary of this first point is that weak stimuli, which are undetectable biochemically because of asynchronicity, e.g. when responses oscillate, or when studying heterogeneous cell populations (i.e. mixed neuronal cultures), become detectable using EGFP–$PH_{PLC\delta}$ translocation. A second advantage is the ability to image both Ins(1,4,5)P_3 production and $[Ca^{2+}]_i$ mobilization in cells dually labelled with EGFP–$PH_{PLC\delta}$ and fura 2. A final point, which although trivial confers a number of real advantages to this technique, is the ability to apply drugs by perfusion and measure Ins(1,4,5)P_3 continuously. This allows for repeated application/removal of drugs over widely variant time frames, while constantly acquiring data. Clearly, this is an extremely attractive approach to study regulation of GPCR-induced responses and to acquire temporal data on Ins(1,4,5)P_3 production.

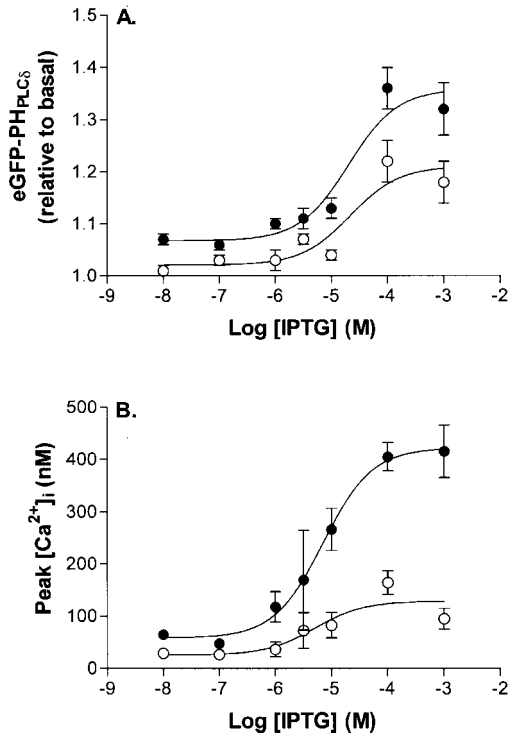

Figure 6 Effect of mGlu1α receptor density on stimulated Ins(1,4,5)P_3 and [Ca^{2+}]$_i$ levels in single CHO-lac-mGlu1α cells

CHO-lac-mGlu1α cells were transiently transfected with EGFP–PH$_{PLC\delta}$ for 48 h and receptor expression induced by incubation with different concentrations of IPTG for 20 h. Cells were then loaded with fura 2 and challenged with 1 mM glutamate and the effect of different mGlu1α receptor density on peak (●) and plateau (○) levels of Ins(1,4,5)P_3 (**A**) and [Ca^{2+}]$_i$ (**B**) in single cells determined. Data are means ± S.E.M. and were compiled from > 6 separate cells from 2–4 experiments.

In conclusion, GPCR-induced translocation of EGFP–PH$_{PLC\delta}$ in single cells offers an excellent method to monitor Ins(1,4,5)P_3 levels in real time. The advantages of this technique over population-based analyses have allowed us to confirm for the first time inferences from earlier biochemical assays on the temporal and graded nature of Ins(1,4,5)P_3 accumulation in single cells. Thus Ins(1,4,5)P_3 levels in individual cells do follow a peak and plateau pattern and responses are dependent on both agonist concentration and receptor density.

We thank the Wellcome Trust for financial support (Programme Grants 16895 and 062495/z/00, and Equipment Grant 061050/z/00) and Professor T. Meyer for his gift of the EGFP–PH$_{PLC\delta}$ construct.

REFERENCES

1 Bootman, M. D., Young, K. W., Young, J. M., Moreton, R. B. and Berridge, M. J. (1996) Extracellular calcium concentration controls the frequency of intracellular calcium spiking independently of inositol 1,4,5-trisphosphate production in HeLa cells. Biochem. J. **314**, 347–354
2 Kawabata, S., Tsutsumi, R., Kohara, A., Yamaguchi, T., Nakanishi, S. and Okada, M. (1996) Control of calcium oscillations by phosphorylation of metabotropic glutamate receptors. Nature (London) **383**, 89–92
3 Parker, I., Choi, J. and Yao, Y. (1996) Elementary events of InsP$_3$-induced Ca^{2+} liberation in Xenopus oocytes: hot spots, puffs and blips. Cell Calcium **20**, 105–121
4 Berridge, M. J. (1997) Elementary and global aspects of calcium signalling. J. Physiol. (Cambridge, U.K.) **499**, 291–306
5 Thomas, D., Lipp, P., Tovey, S. C., Berridge, M. J., Li, W., Tsien, R. Y. and Bootman, M. D. (2000) Microscopic properties of elementary Ca^{2+} release sites in non-excitable cells. Curr. Biol. **10**, 8–15
6 Muallem, S., Pandol, S. J. and Beeker, T. G. (1989) Hormone-evoked calcium release from intracellular stores is a quantal process. J. Biol. Chem. **264**, 205–212
7 Meyer, T. and Stryer, L. (1990) Transient calcium release induced by successive increments of inositol 1,4,5-trisphosphate. Proc. Natl. Acad. Sci. U.S.A. **87**, 3841–3845
8 Oldershaw, K. A., Nunn, D. L. and Taylor, C. W. (1991) Quantal Ca^{2+} mobilization stimulated by inositol 1,4,5-trisphosphate in permeabilized hepatocytes. Biochem. J. **278**, 705–708
9 Bootman, M. D., Cheek, T. R., Moreton, R. B., Bennett, D. L. and Berridge, M. J. (1994) Smoothly graded Ca^{2+} release from inositol 1,4,5-trisphosphate-sensitive Ca^{2+} stores. J. Biol. Chem. **269**, 24783–24791
10 Callamaras, N. and Parker, I. (2000) Phasic characteristic of elementary Ca^{2+} release sites underlies quantal responses to IP$_3$. EMBO J. **19**, 3608–3617
11 Allen, V., Swigart, P., Cheung, R., Cockcroft, S. and Katan, M. (1997) Regulation of inositol lipid-specific phospholipase cδ by changes in Ca^{2+} ion concentrations. Biochem. J. **327**, 545–552
12 Kim, Y. H., Park, T. J., Lee, Y. H., Baek, K. J., Suh, P. G., Ryu, S. H. and Kim, K. T. (1999) Phospholipase C-δ1 is activated by capacitative calcium entry that follows phospholipase C-β activation upon bradykinin stimulation. J. Biol. Chem. **274**, 26127–26134
13 Rebecchi, M. J. and Pentyala, S. N. (2000) Structure, function, and control of phosphoinositide-specific phospholipase C. Physiol. Rev. **80**, 1291–1335
14 Stauffer, T. P., Ahn, S. and Meyer, T. (1998) Receptor-induced transient reduction in plasma membrane PtdIns(4,5)P2 concentration monitored in living cells. Curr. Biol. **8**, 343–346
15 Varnai, P. and Balla, T. (1998) Visualization of phosphoinositides that bind pleckstrin homology domains: calcium- and agonist-induced dynamic changes and relationship to myo-[^{3}H]inositol-labeled phosphoinositide pools. J. Cell Biol. **143**, 501–510
16 Hirose, K., Kadowaki, S., Tanabe, M., Takeshima, H. and Iino, M. (1999) Spatiotemporal dynamics of inositol 1,4,5-trisphosphate that underlies complex Ca^{2+} mobilization patterns. Science (Washington, D.C.) **284**, 1527–1530
17 Kavran, J. M., Klein, D. E., Lee, A., Falasca, M., Isakoff, S. J., Skolnik, E. Y. and Lemmon, M. A. (1998) Specificity and promiscuity in phosphoinositide binding by pleckstrin homology domains. J. Biol. Chem. **273**, 30497–30508
18 Willars, G. B. and Nahorski, S. R. (1995) Quantitative comparisons of muscarinic and bradykinin receptor-mediated Ins(1,4,5)P$_3$ accumulation and Ca^{2+} signalling in human neuroblastoma cells. Br. J. Pharmacol. **114**, 1133–1142
19 Willars, G. B., Challiss, R. A., Stuart, J. A. and Nahorski, S. R. (1996) Contrasting effects of phorbol ester and agonist-mediated activation of protein kinase C on phosphoinositide and Ca^{2+} signalling in a human neuroblastoma. Biochem. J. **316**, 905–913
20 Willars, G. B., Nahorski, S. R. and Challiss, R. A. (1998) Differential regulation of muscarinic acetylcholine receptor-sensitive polyphosphoinositide pools and consequences for signaling in human neuroblastoma cells. J. Biol. Chem. **273**, 5037–5046
21 Hermans, E., Young, K. W., Challiss, R. A. and Nahorski, S. R. (1998) Effects of human type 1α metabotropic glutamate receptor expression level on phosphoinositide and Ca^{2+} signalling in an inducible cell expression system. J. Neurochem. **70**, 1772–1775
22 Hermans, E., Challiss, R. A. and Nahorski, S. R. (1999) Effects of varying the expression level of recombinant human mGlu1α receptors on the pharmacological properties of agonists and antagonists. Br. J. Pharmacol. **126**, 873–882
23 Lambert, D. G., Ghataorre, A. S. and Nahorski, S. R. (1989) Muscarinic receptor binding characteristics of a human neuroblastoma SK-N-SH and its clones SH-SY5Y and SH-EP1. Eur. J. Pharmacol. **165**, 71–77
24 Lambert, D. G. and Nahorski, S. R. (1990) Muscarinic-receptor-mediated changes in intracellular Ca^{2+} and inositol 1,4,5-trisphosphate mass in a human neuroblastoma cell line, SH-SY5Y. Biochem. J. **265**, 555–562
25 Young, K. W., Pinnock, R. D. and Nahorski, S. R. (1998) Determination of the inositol (1,4,5) trisphosphate requirement for histamine- and substance P-induced Ca^{2+} mobilisation in human U373 MG astrocytoma cells. Cell Calcium **24**, 59–70
26 Adkins, C. E. and Taylor, C. W. (1999) Lateral inhibition of inositol 1,4,5-trisphosphate receptors by cytosolic Ca^{2+}. Curr. Biol. **9**, 1115–1118
27 Taylor, C. W. (1998) Inositol trisphosphate receptors: Ca^{2+}-modulated intracellular Ca^{2+} channels. Biochim. Biophys. Acta **1436**, 19–33
28 Wojcikiewicz, R. J., Tobin, A. B. and Nahorski, S. R. (1994) Muscarinic receptor-mediated inositol 1,4,5-trisphosphate formation in SH-SY5Y neuroblastoma cells is regulated acutely by cytosolic Ca^{2+} and by rapid desensitization. J. Neurochem. **63**, 177–185

Received 13 December 2000/12 February 2001; accepted 12 March 2001